Rev. Adv. Mater. Sci. 44 (2016) 257-272

DRUG DELIVERY WITH POROUS SILICON FILMS, MICROPARTICLES, AND NANOPARTICLES

Nalin H. Maniya, Sanjaykumar R. Patel and Z. V. P. Murthy

Department of Chemical Engineering, Sardar Vallabhbhai National Institute of Technology, Surat – 395 007, Gujarat, India

Received: September 30, 2015

Abstract. Porous silicon (PSi) is a nanostructured biomaterial that has received considerable attention for use in a wide variety of biomedical applications, including biosensing, bioimaging, tissue engineering and drug delivery. This interest is due to several key physical and optical properties of PSi, including easy fabrication of porous structure, the ease of surface chemistry modification, excellent *in vivo* biocompatibility, and very low toxicity. With tuning of these properties PSi has successfully been used for the delivery of a variety of therapeutics, ranging from small-molecule drugs to larger peptide/protein-type therapeutics and various anticancer drugs. Drug delivery system of PSi has been developed for mainly two reasons: controlled drug delivery to reduce toxic side effects and to increase oral bioavailability of poorly soluble drugs. The loaded drug releases from porous matrix by either pore diffusion or porous matrix dissolution depending on the pore size and surface chemistry of PSi. This paper reviews the fabrication of PSi by electrochemical etching and other means, and further, surface modifications by oxidation, hydrosilylation, and thermal carbonization. The drug loading into PSi by spontaneous adsorption, covalent attachment, and physical adsorption followed by *in vitro* and *in vivo* release of different drug molecules have then been reviewed.

1. INTRODUCTION

Porous silicon (PSi) was discovered accidentally by Uhlir in 1956 during their experiments on silicon wafers to form smooth polish surfaces by electrochemical method [1]. However, more interest in PSi was developed after the discovery of photoluminescence from PSi by Leigh Canham in 1990s [2]. Furthermore, canham addressed the biocompatibility, resorbability, and toxicity of PSi during same time period [3-5]. Since then, PSi has been exploited for numerous applications including, optical chemical and biosensing [6-9], bioimaging [10,11], biomolecular screening [12], tissue engineering [13], and drug delivery [14-18].

PSi based drug delivery systems may be prepared in the form of films or particles by electrochemical etching of single crystalline silicon wafers. The desired optical and physical properties can be obtained by varying etching parameters such as current density and time. A very high surface area to volume ratio [19], ease in surface modification [20], controllability in pore size and volume [19,21], real time monitoring [22], and biocompatibility [23,24] of PSi makes it an excellent biomaterial for drug delivery applications. PSi easily degrades into nontoxic orthosilicic acid which can be excreted through the urine and PSi particles have shown no toxicity into the rabbit or rat eye [25-27].

In this review, we will start with PSi fabrication by electrochemical etching and other methods followed by particles preparation. Different surface modifications and drug loading procedures of PSi are also reviewed. Furthermore, a special focus is

Corresponding author: Z. V. P. Murthy, e-mail: zvpm2000@yahoo.com, zvpm@ched.svnit.ac.in

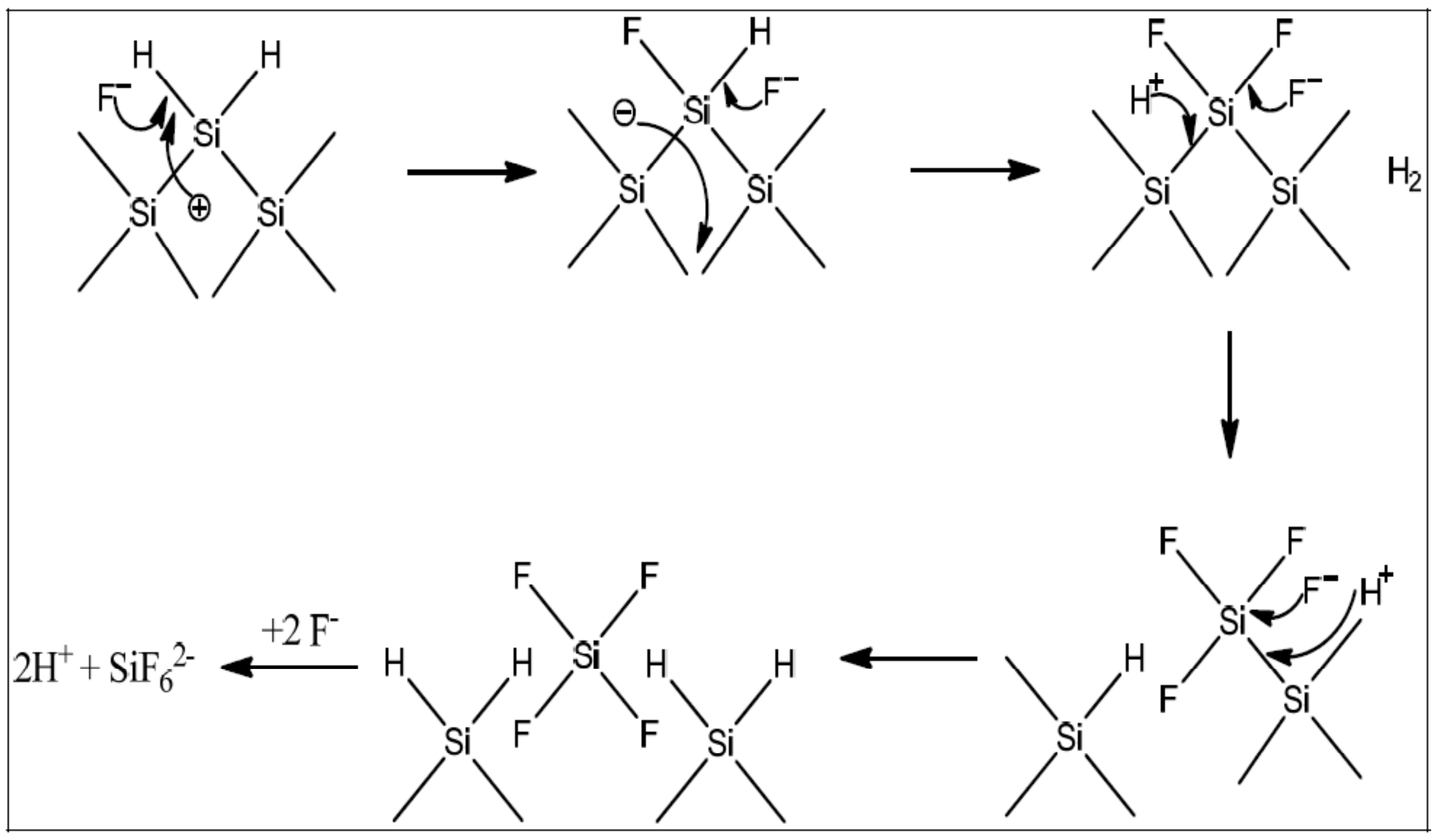

Fig. 1. Mechanism of Si dissolution during the formation of PSi.

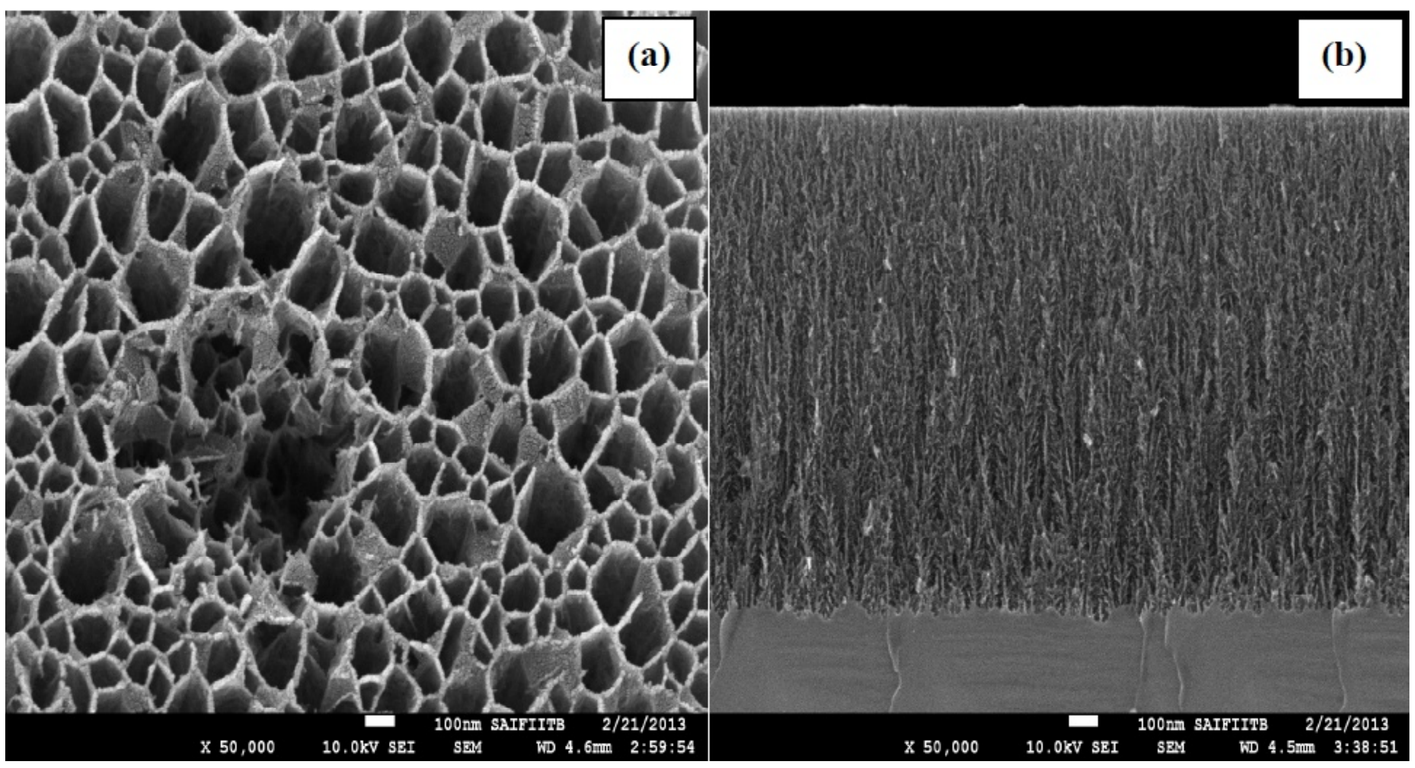

Fig. 2. SEM images of (a) plan view and (b) cross section of the p^+ type PSi.

given to *in vitro* and *in vivo* delivery of different drug molecules using PSi films, micro- and nanoparticles.

2. FABRICATION OF PSi

PSi is most frequently prepared by electrochemical etching of silicon wafers in hydrofluoric acid (HF) based electrolytes [1]. However, several other methods such as stain etching [28,29], photochemical etching [30,31], gas, vapour, and spark induced etching [32-34] have also been investigated. In electrochemical etching, a current is applied to the silicon wafer working as anode and a cathode (usually made of platinum) in a HF based solutions. The etching is carried out in etching cell typically made up of acid resistant material such as Teflon. Ethanol is added as a surfactant in the electrolyte to reduce the formation of hydrogen bubbles, to improve the electrolyte penetration in the pores, and to prepare uniform PSi layer. Silicon wafers with either boron doped (p- type) or phosphorus doped (n- type) are used to fabricate PSi.

The mechanism of pore formation is still not completely understood, but it is generally accepted that valence band holes are required in the initial steps for both pore formation and electropolishing [19]. The widely accepted model for pore formation in silicon during electrochemical etching in HF was proposed by Lehmann and Gosele [35,36] and is shown in Fig. 1.

During electrochemical etching, hole reaches hydrogen terminated surface of silicon due to applied anodic current and a nucleophilic attack of the Si-H bonds by fluoride ions takes place resulting in the formation of Si-F bond. The formed Si-F bond exerts a polarising influence resulting in another F^- ion bonds to the silicon with the generation of an H_2 molecule and the injection of one electron into the electrode. The polarization induced by the two Si-F bonds weakens the Si-Si backbonds that are easily attacked by HF or H_2O, in presence of a second hole, in a way that the silicon surface atoms remain bonded to fluoride atoms. The unstable silicon tet-

rafluoride molecule reacts with two equivalents of F^- in solution to form the highly stable SiF_6^{2-}. For n-type silicon wafers where holes are minority carriers, the electrochemical dissolution of the silicon substrate strongly depends on the hole/electron pair generation by illumination [37].

The pore diameters of porous materials are classified into three different size groups: micropores (< 2 nm), mesopores (2-50 nm), and macropores (> 50 nm). Pores of different sizes from micro to macropores ranging 1 nm to few microns can be easily prepared by varying current density, electrolyte concentration, type and concentration of dopant (p-type or n-type), and crystalline orientation of Si wafer [38]. Furthermore, pores with smooth walled or branched, interconnected or independent can be easily prepared. Fig. 2 shows the scanning electron microscopy (SEM) images of PSi prepared using p^+-type Si wafer.

The pore diameters increase with an increase in dopant concentration and decrease in resistivity. Furthermore, type of dopant also affects pore diameters as n-type Si gives larger pores than p-type Si [39]. However, this pore diameter depends on the current density and illumination parameters, for example, wavelength of illumination and intensity in the case of n-type Si [40,41]. The pore diameter also increases with increase in the current density and decrease in HF concentration [21,42]. The surface area of PSi can be modulated from few m^2/g to 1000 m^2/g by varying the etching parameters. The surface area increases with increase in HF concentration and decreases with increase in current density and etching time. The resistivity of Si wafer also influences surface area with decrease in surface area is observed by decreasing the resistivity [42].

It has been determined that porosity and thickness of porous layer increases with increase in current density and etching time, respectively [21]. Porosity can be varied from 5 to 95% by controlling current density. The change in current density results in change in porosity which allows fabrication of complex layered structures such as one-dimensional photonic crystal consisting of a stack of layers with alternating refractive index [43-46]. The electrochemical etching provides easy fabrication procedure for tuning of pore sizes and volumes for drug delivery applications. PSi with larger pores can be fabricated with larger current density for loading and release of sizable drug molecules, whereas small pores can be obtained for loading of small drug molecules. Porosity and pore size also affects degradation rates of porous matrix in aqueous media [47]. PSi with small pores yield large surface area and degrades easily than larger pores.

Stain etching is the second most popular method after electrochemical etching for the fabrication of PSi. This process involves purely chemical reaction consisting of HF and nitric acid in place of power supply which produces brownish or reddish color PSi film [28,29]. The pore formation occurs due to the NO (nitric oxide) which serves as a hole injector is produced by the cathodic reaction of HF and nitric acid. Stain etching is a simpler method than electrochemical etching due to the no requirement of power supply. However, stain etching cannot be used for fabrication of multilayer structures and reproducibility is less compared to electrochemical etching process.

The morphology of prepared PSi, for example, porosity, pore size, and thickness can be easily characterized by several destructive and non-destructive methods. The porosity and thickness of PSi film can be obtained by destructive gravimetric method. In this method, weights of PSi sample before etch, after etch, and after dissolving porous layer in basic aqueous solutions (KOH or NaOH) are used to determine porosity and thickness. Such morphology can also be determined by non-destructive method called spectroscopic liquid infiltration method (SLIM) developed by MJ sailor [48,49]. SLIM uses reflectance property of PSi to determine porosity and thickness. In this method, reflectance spectra of PSi film held in the air and in liquid of a known refractive index are measured. Liquid infiltration into the pores changes the average refractive index of the PSi film and results in a shift in the reflectance spectrum. Then Fourier transformations of the reflectance spectra are carried out using software to determine effective optical thickness (i.e. $2nL$) of film. These optical thickness values are then fit into the two component effective medium approximation. However, both gravimetric and SLIM has limitations and accurate determination of porosity and thickness is not possible.

The pore size, porosity, and thickness can be accurately measured by high resolution scanning electron microscopy and transmission electron microscopy. Pore morphologies may also determined by atomic force microscopy and scanning tunneling microscopy. Pore size, pore size distribution, porosity, and specific surface area can be calculated by BET (Brunnauer-Emmett-Teller), BJH (Barret-Joyner-Halenda), and BdB (Broekhof-de Boer) methods by measuring nitrogen sorption isotherms [50]. SEM and nitrogen sorption measure-

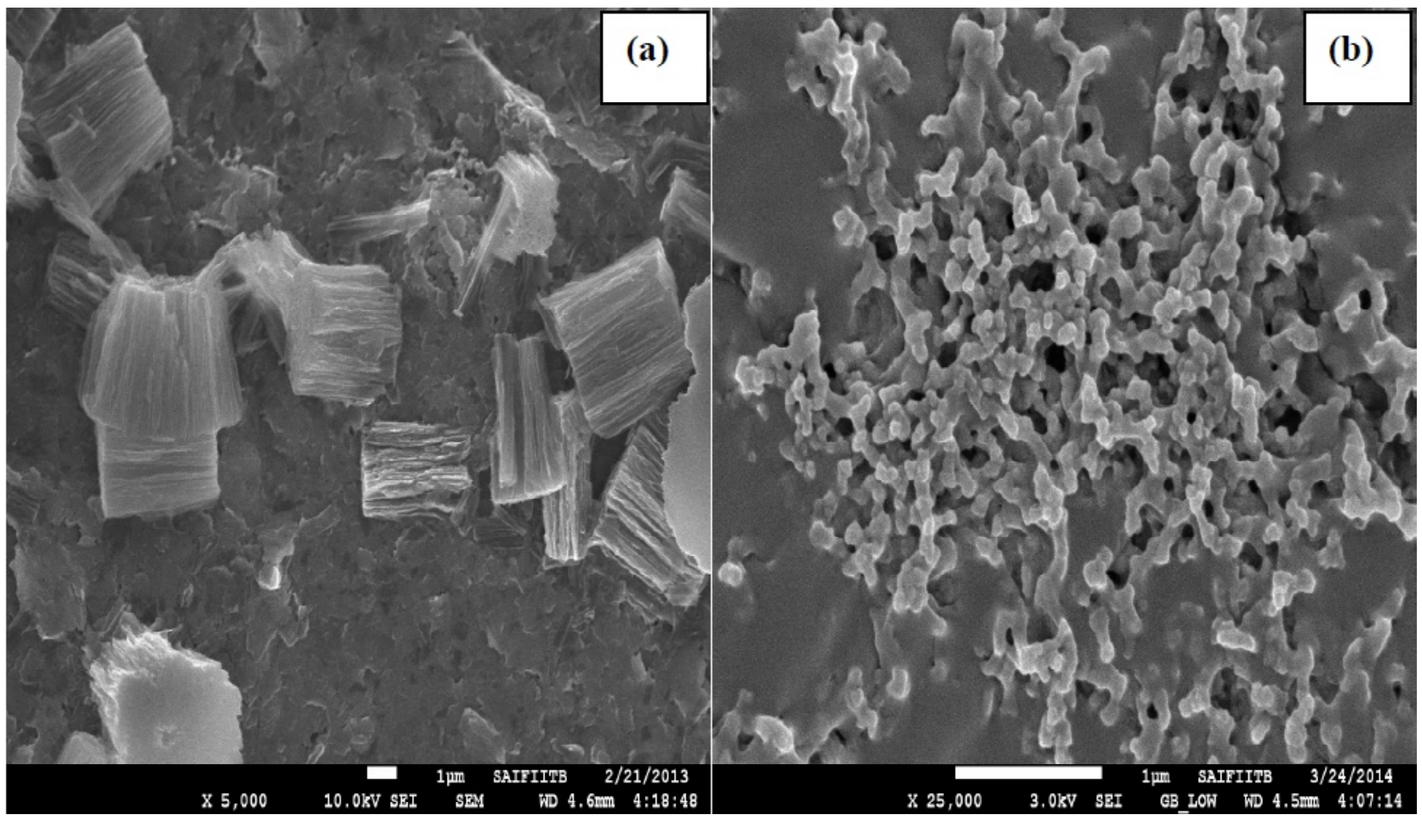

Fig. 3. SEM images of PSi (a) micro and (b) nanoparticles prepared by ultrasonic fracture of freestanding films.

ments should be used to determine accurate morphology of PSi.

3. PREPARATION OF PSi MICRO- AND NANOPARTICLES

Electrochemical etching of silicon wafer produces PSi film, which is required to remove from the silicon substrate and break into particles for *in vivo* applications. The PSi film can be removed by electropolishing (lift-off) process using low concentration of HF and by applying current density for several seconds. The mechanism behind electropolishing is the formation of SiO_2 instead of SiF_4 due to the low concentration of HF. The SiO_2 layer then dissolves in HF and separates from silicon substrate [19].

The freestanding films can be fractured by ultrasonication, ball milling, or jet milling into micro- or nanoparticles. For ultrasonic fracture, films are placed in ethanol or other solvent and sonicated in ultrasonic bath for several minutes to hours to prepare micro- and nanoparticles; respectively (Fig. 3) [51]. The applied ultrasonic time duration and solvent used for fracture determines the size of particles. However, these techniques produce particles of irregular shape and wide size distributions from tens of nanometers to several micrometers. The particles can then be sieved or centrifuged to obtain desired size. The particles with uniform size can be prepared by introducing high porosity layers in regular porosity layers [52,53]. The particles with uniform shapes can also be produced by expensive lithography or microdroplet patterning methods [54,55].

4. CHEMICAL MODIFICATION OF PSi SURFACE

Surface chemistry plays an important role in drug loading, drug release and degradation of PSi matrix. The freshly etched PSi surface is hydride terminated (Si-H, $Si-H_2$, and $Si-H_3$) and slowly aged in ambient air, thereby affects both its structural and optoelectronic properties. The aging of native PSi occurs due to the oxidation of surface and depends on environmental conditions, such as temperature, humidity, air composition, etc. [56]. Different impurities, for example, oxygen, carbon, and fluorine are also observed shortly after PSi fabrication. Furthermore, an unstable surface of native PSi has been found to be reactive with several drugs [57,58]. Therefore, chemical modification of native surface is required to stop aging and further stabilize the PSi. The three most commonly used treatments for the stabilization of PSi are the oxidation, hydrosilylation, and thermal carbonization.

4.1. Oxidation of PSi

PSi oxidation can be carried out in several ways, for example, thermal, photo, anodic, and chemical oxidations. Different organic and inorganic agents such as ozone, dimethyl sulfoxide, and pyridine have been used for the oxidation of PSi [59-61]. Thermal oxidation is a simple method to stabilize PSi surface. Partially oxidized surface can be obtained by heating PSi in air at 300 °C for few hours and complete oxidation of surface takes place at 900 °C. The partial oxidation incorporates oxygen into the Si-Si bonds resulting in the formation of backbonded species. However, as oxidation temperature in-

creases these backbonded species gradually diminish and completely removed by oxidation at 600 °C [62, 63]. Thermal oxidation is, however, decreases the pore diameter, porosity, and specific surface area due to the structural expansion. Thermal oxidation also converts hydrophobic surface of native PSi into hydrophilic which is useful for loading and release of many hydrophilic drugs.

4.2. Hydrosilylation of PSi

PSi hydrosilylation occurs by thermal, photochemical, or Lewis acid catalysts via the reaction of surface Si-H species with alkenes, alkynes, or aldehydes [20,64-69]. This reaction replaces Si-H bonds with Si-C bonds which is useful to increase stability and to attach a wide variety of functional groups for use in applications such as; drug delivery [22,26,57], chemical sensors [70], and biosensors [71]. The hydrosilylation reaction produces Si-C surface which possess higher kinetic stability due to the low electronegativity of carbon in comparison to Si-O surface.

Thermal hydrosilylation is frequently carried out by immersing hydrogen terminated PSi into neat alkene using microwave radiation [64,66]. Microwave-assisted hydrosilylation not only provides stable Si-C surface, but also allows the introduction of a wide variety of functional groups on a PSi surface. This reaction gives a higher surface coverage due to the high energy of microwaves and very high treatment efficiency has been reported [65]. Furthermore, hydrophilic surface can be prepared by reaction of undecylenic acid with PSi for drug delivery applications. This reaction takes place between Si-H groups and terminal alkene, and therefore, freshly etched PSi should only be used. Different organic compounds, for example, dodecene, undecylenic acid, methoxy, trimethylsiloxy, and folate are used for the hydrosilylation of PSi [22,57,65,66,72-74].

PSi surface modifications can be done by chemical or electrochemical grafting techniques using Grignard, alkyl, or aryllithium reagents [75-78]. Dense monolayers covalently attached to the PSi and single crystal Si have been prepared by the electrochemical oxidation of methyl-Grignards and electrochemical reduction of phenyldiazonium salts, respectively [79,80]. Organohalides also produces Si-C bonds by the cleavage of Si-H bonds due to the electrochemical reduction which improves the stability of the surface [81]. Grafting technique is an alternative to hydrosilylation; however, it allows the attachment of methyl group which is not possible with the hydrosilylation technique. Hydrosilylation and grafting techniques produce stable surfaces with coverage of 20-80% which means Si-H groups still remaining on the surface after treatment. The Si-H groups can be completely removed by methylation using CH_3I on the functionalized surface to form a completely Si-C terminated surface [82].

4.3. Thermal carbonization of PSi

Salonen and coworkers have extensively investigated thermal carbonization of PSi since year 2000 [83-85]. Thermal carbonization produces more stable Si-C surface than those produced by thermal oxidation and very high surface coverage can be obtained. Although thermal oxidation produces stable surface, the Si-O bonds are susceptible to hydrolytic attack in aqueous solutions. On the contrary, Si-C surface produced by thermal carbonization is stable in humid atmospheres and harsh chemical environments [86].

Thermal carbonization is carried out using acetylene vapour to from carbonized PSi that is very stable and chemically inert. This process involves initial acetylene vapour flush followed by thermal treatment. The temperature in thermal treatment is responsible for surface groups produced and two different surface terminations can be obtained. Thermally hydrocarbonized PSi is produced by constant flow of acetylene and nitrogen gas and then heating at temperature less than 700 °C. This PSi surface contains Si-H species like hydrosilylated PSi and therefore is hydrophobic. The second type of surface terminations with completely carbonized PSi can be formed by heating at temperature above 700 °C after acetylene flow stopped. The completely carbonized PSi is highly stable in acidic as well as basic solutions and has been found to be inert in chemically harsh environments [87]. This high stability is particularly important for loading of highly reactive drug molecules and implantable drug delivery applications. Furthermore, thermal carbonization of PSi results in lesser decrease in surface area in comparison to thermal oxidation. However, thermally oxidized PSi without any chemical species is less likely to produce any toxic side effects and can be used for short term (minutes to hours) drug delivery applications. On the other hand, thermally hydrosilylated PSi or thermally carbonized PSi is preferred when long term or extended drug release is required.

4.4. Biofunctionalization of PSi

For biological applications, biofunctionalization of PSi surface after stabilization is required to minimize biocompatibility issues, to target PSi nanoparticles to diseased sites, and to deliver drugs. The thermally hydrosilylated PSi with undecylenic acid can be easily functionalized by coupling reagent 1-ethyl-3-[3-dimethylaminopropyl] carbodiimide hydrochloride (EDAC) for loading of primary amine containing drug molecules [22,57]. Biocompatibility of stabilized PSi can be improved by attachment of polyethylene glycol (PEG) linker to the surface which avoids non-specific binding of unwanted proteins and other interfering species [88-90]. Thermally oxidized PSi can be functionalized by using conventional silanol chemistries [89]. A coupling reagent 3-aminopropyltriethoxysilane is frequently used to attach proteins, DNA, and many other molecules to the oxidized PSi surfaces [90,91]. Both monoalkoxydimethylsilanes and trialkoxysilanes are used for functionalization of PSi. However, monoalkoxydimethylsilanes is preferred over trialkoxysilanes when functionalization of microporous sample is required because trialkoxysilanes clog smaller pore openings of microporous samples [92].

5. BIOCOMPATIBILITY AND BIODEGRADABILITY

PSi has been extensively studied for biomedical applications especially as a drug delivery carrier due to its biocompatibility, biodegradability, low toxicity and solubility [3-5,23,24]. PSi has shown good biocompatibility in biological systems without causing any undesirable side effects. The first biocompatibility study of PSi was carried out by Canham [3], and then a lot of work addressing *in vitro* and *in vivo* biocompatibility study of PSi, for example, calcification [3-5], cell adhesion [23,93], protein binding [94], and tissue biocompatibility [95] has been carried out. PSi has been found to be biodegradable material which dissolves in biological fluids. The degradation product of PSi is a non-toxic orthosilicic acid ($Si(OH)_4$), which is naturally found in numerous tissues and can be absorbed by the human body or excess readily excreted by kidneys [25-27]. In addition, PSi has been found to support growth of several cell types including osteoblasts, neurons, and hepatocytes [13,96,97].

$$SiH_4 + 2H_2O \rightarrow SiO_2 + 4H_2, \quad (1)$$

$$Si + O_2 \rightarrow SiO_2, \quad (2)$$

$$SiO_2 + 2H_2O \rightarrow Si(OH)_4. \quad (3)$$

Low et al. [27] studied the biocompatibility of thermally-oxidised and aminosilanised PSi membranes *in vitro* and *in vivo*, in the rat eye. They observed thin fibrous capsule surrounding the implant with no erosion of the surrounding tissue, inflammatory response, or neovascularization. Park et al. [98] showed good *in vivo* biocompatibility of luminescent PSi nanoparticles with very low toxicity. The nanoparticles injected intravenously into mice were observed to accumulate mainly in liver, kidney, and spleen. The particles were degraded *in vivo* into apparently non-toxic products within a few days and removed from the body through renal clearance.

The biocompatibility of PSi has been found to be dependent on porosity, pore size, and surface chemistry of PSi. The highly porous PSi ($p > 70\%$) easily degrades in simulated biological fluids while PSi with low porosity ($p < 70\%$) degrades slowly and is found to be bioactive. Surface chemistry has profound effect on biodegradability of PSi [17].

Tolli et al. [99] also demonstrated good *in vivo* biocompatibility of different sizes of thermally hydrocarbonized PSi microparticles and thermally oxidized PSi micro and nanoparticles in the rat heart tissue to develop drug delivery carriers for heart. Both particle types showed no cytotoxicity, however, *in vivo* inflammation and fibrosis promoting responses was different for thermally hydrocarbonized and thermally oxidized PSi particles. For example, thermally hydrocarbonized microparticles exhibited greater activation of inflammatory cytokine and fibrosis promoting genes compared to thermally oxidized PSi particles.

Santos et al. [100] studied the *in vitro* cytotoxicity of PSi particles with different surface chemistry, particle size and concentration on the Caco-2 cells. Smaller particles (diameters between 1 and 25 μm) showed higher cytotoxicity compared with larger particles. Furthermore, thermally oxidized PSi was found to be less cytotoxic than thermally carbonized or hydrocarbonized PSi.

6. DRUG LOADING

Drug loading into PSi films and micro- or nanoparticles is carried out by either immersion or impregnation method. In the immersion method, PSi films or particles are immersed in drug loading solution containing desired drug molecule dissolved in appropriate solvent [16,22]. This is a simple

method, however, requires higher amount of drug molecules. For impregnation method, controlled amount of drug loading solution is used for loading of films and particles [24]. The benefit of this method is less amount of drug required for loading. Furthermore, impregnation method can be applied for loading of small amounts of sample. Drug loading into PSi is affected by several factors including pH of solvent, temperature, time, and chemical reactivity of PSi to the drug loading solution. Also, choice of solvent, interactions between the drug and PSi, the drug and the solvent, the solvent and PSi, and the drug concentration affects drug loading process.

Drug loading of PSi can be grouped into following three categories: spontaneous adsorption, covalent attachment, and physical trapping.

6.1. Spontaneous adsorption

The surface chemistry plays important role in drug loading and release behaviour. The surface of native PSi is hydrophobic due to the hydride species present on the surface while oxidized PSi is hydrophilic. The surface of thermally carbonized PSi can be hydrophobic or hydrophilic depending on treatment conditions. These surface species extract drug molecules from loading solution and holds on porous matrix due to electrostatic adsorption. The spontaneous adsorption loads drug weakly than covalent attachment and physical trapping and therefore can be used for more rapid drug delivery [47]. The surface of thermally oxidized PSi has negatively charged surface that can be used for loading of positively charged drug molecules by spontaneous adsorption [98].

6.2. Covalent attachment

Covalent attachment approach for drug loading can be applied when sustained drug release behaviour for a period of days, weeks or months is required [22,26,57]. This sustained release is observed due to the more stable Si-C bonds than Si-O bonds used in spontaneous adsorption for drug loading. Thermal hydrosilylation and thermal carbonization produce Si-C bonds which are very stable in aqueous solutions. The PSi hydrosilylation with undecylenic acid attaches a hydrophobic aliphatic chain to the surface [66]. This surface produces stable Si-C chemistry which can be used directly or after PEG attachment for drug loading [89]. The drug attaches so strongly to the surface that release can only possible when covalent bond breaks or porous matrix is degraded.

6.3. Physical trapping by oxidation

In this method, drug is loaded into the porous matrix and then trapping of loaded drug is carried out by oxidation. The oxidation of PSi results in volume expansion due to the incorporation of oxygen atoms in silicon skeleton which shrink the pores and causes trapping of drugs molecules present in the pores. The oxidation can be induced by nitrite, peroxide, dimethyl sulfoxide, ammonia, or pyridine for physical trapping of drug molecules [60,101-105]. The PSi matrix needs to be fabricated in such way that drug molecules easily diffuses into the pores during loading and do not diffuse out of the oxidized pores. This approach for loading particularly has limitations for loading of more sensitive protein, drugs, and oligonucleotide therapeutics. In a recent study, drug molecules trapped by oxidation of PSi using sodium nitrite showed increased drug loading and sustained release compared to the drug loaded by adsorption [106].

7. DRUG RELEASE

Drug delivery system of PSi has been developed for mainly two reasons: controlled drug delivery to reduce toxic side effects and to increase oral bioavailability of poorly soluble drugs. The loaded drug releases from porous matrix by either pore diffusion or porous matrix dissolution depending on the pore size and surface chemistry of PSi. Drug release study has been carried out from PSi films [107-109], particles [11,16,22,24,57], chip implants [110], composite materials [111-113], and microneedles [114]. The PSi microneedles have been fabricated for implantable drug delivery [114,115]. PSi films and micro- or nanoparticles can be easily prepared by less expensive and less time consuming electrochemical etching while chip implants and other sophisticated structures are produced by microfabrication techniques. PSi films and micro- and nanoparticles have already been studied for incorporation and release of small drug molecules [16,18,108,116-123], anti-cancer agents [22,57,98,109,111,112], peptides, proteins [24,58], and small interfering RNA [124].

7.1. Small molecule drug delivery

The oral drug delivery route is most widely and preferred route for the administration of drug molecules due to its patient compliance. However, many drug molecules especially poorly soluble drugs suffer from low oral bioavailability due to the poor dissolution in gastrointestinal tract, poor permeation across the

intestinal wall, and extensive pre-systemic metabolism in the gut and liver. PSi can be used to increase dissolution of poorly soluble drugs for oral drug delivery applications. PSi micro- or nanoparticles with desired pore size can be fabricated so that drug remains in pores in amorphous form. Because of the amorphous or disordered state higher dissolution rates can be achieved than its crystalline form. Furthermore, dissolution rates are increased due to the very high surface area of PSi particles [16,116].

Salonen et al. [16] prepared mesoporous silicon microparticles with thermally oxidized and thermally carbonized surfaces for oral drug delivery of poorly soluble drugs ibuprofen, griseofulvin, and furosemide and soluble drugs antipyrine and ranitidine. They showed improved dissolution of poorly soluble drugs and delayed release with higher dissolution rate of soluble drugs after loading into microparticles. Kaukonen et al. [117] studied the combined release and permeation behavior of furosemide loaded into thermally carbonized PSi particles. Permeation was investigated across Caco-2 monolayers at different pH from drug solutions and thermally carbonized particles. Particles loaded with furosemide exhibited improved dissolution with greatly diminished pH dependence. Furthermore, permeation across Caco-2 monolayers was increased over fivefold at pH 5.5 and over fourfold at pH 6.8 and pH 7.4 compared to pre-dissolved furosemide. Bimbo et al. [118] investigated the behaviour of thermally oxidized PSi micro- and nanoparticles loaded with griseofulvin in Caco-2 epithelial cells and RAW 264.7 macrophages. The results showed that micro and nanoparticles do not permeate across the differentiated Caco-2 cell monolayers, even after 24 hours of incubations but were readily internalized by the RAW 264.7 macrophages. Furthermore, griseofulvin loaded nanoparticles improved the drug permeability across the differentiated Caco-2 cell monolayers.

The surface chemistry and pore size of PSi carriers greatly affect drug loading and release in oral drug delivery applications. Different surface chemistries prepared by, for example, thermal oxidation and thermal carbonization not only stabilizes the particles but also determines the affinity of drugs to the surface. In order to study the effect of surface chemistry and pore size on PSi properties as drug carriers, Limnell et al. [119] prepared six different types of mesoporous silicon microparticles. The studied PSi particles were as-anodized, thermally carbonized, thermally oxidized, annealed thermally carbonized, annealed thermally oxidized, and thermally hydrocarbonized PSi. The loading of poorly soluble drug ibuprofen into PSi particles improved the dissolution rates in all the studied chemistries. However, thermally carbonized PSi showed fastest dissolution due to the small pore size and most stable surface of particles. The small pore size retained drug in amorphous form which dissolves faster than its crystalline form. The thermally oxidized PSi particles displayed dissolution rate slower than thermally carbonized particles as drug resides on the surface of thermally oxidized particles in crystalline form decreases dissolution rate. In addition, annealed thermally hydrocarbonized particles with big pore size showed slower dissolution rate than thermally hydrocarbonized particles whereas annealed thermally oxidized particles showed faster release in compared to thermally oxidized particles.

Indomethacin was loaded into oxidized PSi microparticles by immersion or solvent evaporation for oral drug delivery applications. The bioavailability of indomethacin was increased and accelerated immediate release with enhanced oral delivery performance of indomethacin was observed in comparison to its crystalline counterpart [120]. In a recent study, indomethacin loaded oxidized PSi microparticles were formulated into tablets and its dissolution and permeation properties were evaluated [121]. The tablets containing indomethacin loaded PSi particles showed enhanced dissolution and permeation of indomethacin across Caco-2 cell monolayers compared to the bulk indomethacin tablets.

Kinnari et al. [122] prepared thermally oxidized and thermally carbonized mesoporous silicon and non-ordered mesoporous silica microparticles in order to enhance dissolution properties of poorly soluble drug itraconazole. Incorporation of itraconazole in both microparticles enhanced the solubility and dissolution rate of the drug, compared to the pure crystalline drug.

Ethionamide, a thioamide antibiotic and one of the most widely used drugs as second line agent for the treatment of tuberculosis has been loaded into the thermally carbonized PSi microparticles to improve the bioavailability. The solubility and permeability of ethionamide were enhanced after loading into PSi particles at different pH-values. Ethionamide was in general toxic at concentrations above 0.50 mM to HepG2, Caco-2, and RAW macrophage cells, but the toxicity was drastically reduced when the drug was loaded into the microparticles [123].

A steroid dexamethasone was also loaded into freshly etched and hydrosilylated PSi film for con-

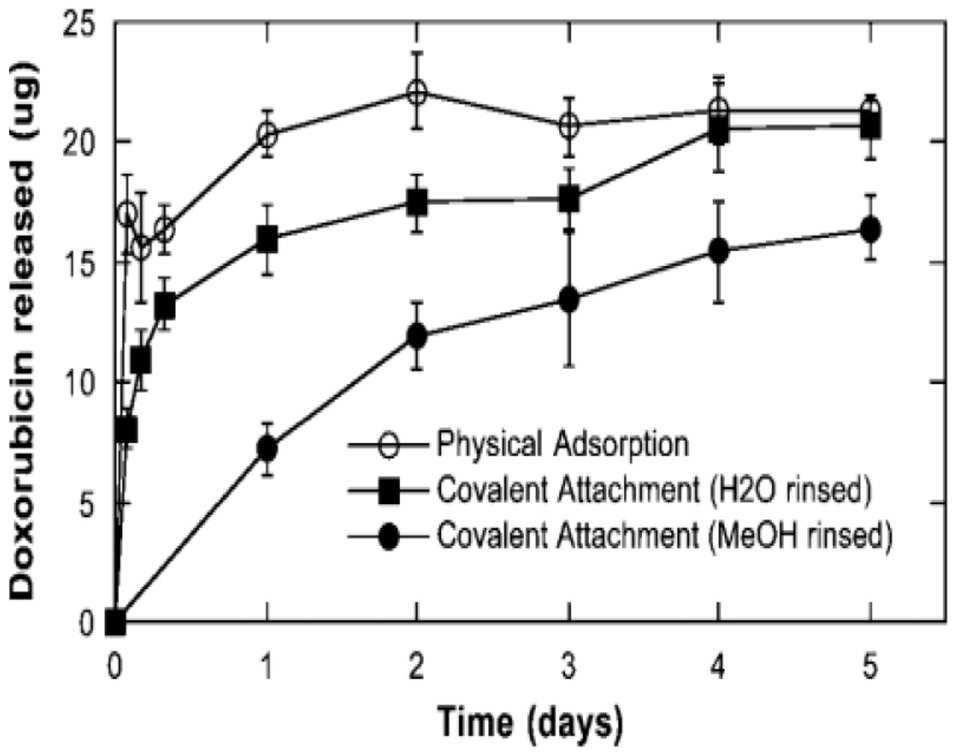

Fig. 4. Release of doxorubicin from PSi microparticles into phosphate buffer saline buffer, Reproduced with permission from E.C. Wu, J.H. Park, J. Park, E. Segal, F. Cunin and M.J. Sailor // *ACS Nano* **2** (2008) 2401, (c) 2008 American Chemical Society).

trolled release behaviour [108]. Dexamethasone release from freshly etched samples occurs much more rapidly than from the hydrosilylated films. The faster release can be attributed to the increased rate of degradation of fresh PSi in phosphate buffered saline solutions. The freshly etched films displayed a linear release of drug over 2 hours, while the stable hydrosilylated PSi film showed a linear release profile for the first 2 hours followed by a slower release period of up to 3 days.

Sustained delivery system of antiviral [18,125], antibacterial [126], and antifungal [127] compounds has also been investigated using PSi carriers to improve the oral bioavailability. Saliphenylhalamide, a potent antiviral compound against influenza A virus was loaded into the thermally hydrocarbonized PSi nanoparticles to improve its poor water solubility, reduce side effects, and increase bioavailability. *In vitro* saliphenylhalamide release from PSi nanoparticles into human retinal pigment epithelium and Madin-Darby canine kidney cells displayed excellent *in vitro* stability, low cytotoxicity, reduction of viral load, and increased dissolution [125]. Acyclovir was loaded into the surface modified PSi micro- and nanoparticles and its *in vitro* release behaviour in phosphate buffered saline was studied. *In vitro* study showed burst release from native and thermally oxidized particles and continuous and slower release from thermally hydrosilylated PSi particles [18]. Antibacterial compound triclosan loaded into the nanostructured mesoporous silicon demonstrated sustained inhibition of bacterial growth for more than 100 days [126]. Mesoporous silicon particles loaded with antifungal drug ketoconazole also showed sustained antifungal activity for as long as 130 days [127].

7.2. Protein and peptide delivery

Proteins and peptides are promising but challenging molecules for drug delivery because of poor oral bioavailability and restricted administration routes. In addition, they are typically administered parenterally either in solutions or in particulate drug delivery systems due to their large molecular size, chemical characteristics and sensitivity to breakdown in the gastrointestinal tract. The bioactivity of protein is determined by its structure which can be maintained by loading proteins into PSi carriers. PSi has been successfully employed for loading and release of proteins and peptides for example insulin, human serum albumin, papain, Melanotan II, peptide YY3-36, ghrelin antagonist, and Glucagon like peptide-1 (GLP-1) [24,58,128-135].

Foraker et al. [24] fabricated PSi microparticles for loading and release of insulin across intestinal Caco-2 cell. The permeation enhancer sodium laurate with different doses was used with insulin for loading of particles. Insulin loading into PSi microparticles resulted in 10-fold higher flux across Caco-2 cell monolayers in compared to liquid formulations with permeation enhancer and up to 100-fold compared with liquid formulations without enhancer.

GLP-1 was loaded into the three nanosystems composed by three different biomaterials (poly(lactide-co-glycolide) polymer (PLGA), Witepsol E85 lipid (solid lipid nanoparticles, SLN) and PSi to study their permeability *in vitro* [135]. Among all the nanosystems, PLGA and PSi were the only nanoparticles able to sustain the release of GLP-1 in biological fluids when coated with chitosan. This characteristic was also maintained when the nanosystems were in contact with the intestinal Caco-2 and HT29-MTX cell monolayers. The chitosan-coated PSi nanoparticles showed the highest GLP-1 permeation across the intestinal *in vitro* models.

Thermally hydrocarbonized PSi microparticles have been loaded with peptides Melanotan II (MTII) and ghrelin antagonist (GhA) [130]. *In vivo*, MTII loaded PSi induced an increase in the heart rate 2 hours later than MTII solution, and the effect lasted 1 hour longer. In addition, MTII loaded PSi changed the water consumption after 150 minutes, when the immediate effect of MTII solution was already diminished. *In vitro* studies in phosphate buffered

saline indicated sustained release of MTII from the PSi microparticles. GhA loaded thermally hydrocarbonized PSi microparticles inhibited food intake for a prolonged time and increased blood pressure more slowly than encountered with a GhA solution. Furthermore, PSi microparticles did not increase cytokine activity.

Peptide PYY-36 has been loaded into thermally oxidized, undecylenic acid-treated thermally hydrocarbonized, and thermally hydrocarbonized PSi nanoparticles for sustained subcutaneous and intravenous delivery [131]. The route of administration was found to affect drastically in peptide release from the PSi nanocarriers in mice. Subcutaneous nanocarriers are demonstrated to be capable of sustaining PYY3-36 delivery over 4 days. The pharmacokinetic parameters of PYY3-36 were presented to be similar between the subcutaneous PSi nanocarriers despite surface chemistry. In contrast, intravenous delivered PSi nanocarriers display significant differences between the surface types. Peptide PYY-36 was also co-loaded with hydrophobic drug indomethacin into PSi for multi drug delivery applications [132]. Drugs loading into the PSi resulted in enhanced drug release rate of each drug and their amount permeated across Caco-2 and Caco-2/HT29 cell monolayers with very high drug loading degrees.

7.3. Anti-cancer drug delivery

Anti-cancer drugs cisplatin [136,137], doxorubicin [98,138,139], daunorubicin [22,57,111,140-142], camptothecin [112], and mitoxantrone dihydrochloride [109] have also been incorporated into surface modified PSi. Cisplatin was loaded into PSi by applying a cathodic bias to the PSi segment placed in cisplatin/simulated body fluid electrolyte. The loading of PSi wafer structures was increased by increasing concentration of cisplatin in the simulated body fluid solution from 1 mM to 3 mM. The amount of cisplatin released reached equilibrium after 10 hours, with this amount remains constant for over 70 hours [136]. PSi microparticles with dodecene and undecylenic acid hydrosilylated surfaces were loaded with cisplatin via trapping with metallic platinum. PSi hydrosilylated using dodecene did not demonstrate significant cisplatin loading due to its hydrophobic surface. Cisplatin loaded hydrosilylated PSi showed higher toxicity towards human ovarian cancer cells than free cisplatin [137].

Doxorubicin was also loaded into hydrosilylated PSi microparticles by covalent attachment. Drug release profiles from covalently attached doxorubicin and water or methanol rinsed was compared with physically adsorbed (Fig. 4). PSi microparticles loaded with doxorubicin through physical adsorption demonstrated burst release within the first 2 hours and complete release within 24 hours. Particles with water rinsed displayed a smaller initial burst followed by a gradual release over a period of 24 hours while particles with methanol rinsed did not exhibit initial burst release, but continuous slow release over 5 days. This slower release behaviour without burst effect is attributed to the removal of all physisorbed drug after methanol rinse [139]. A controlled and observable drug delivery system of daunorubicin has been developed using PSi photonic crystal microparticles. Thermally hydrosilylated PSi microparticles using 1-undecylenic acid attaches daunorubicin to the carboxy terminus of the linker. The sustained release of daunorubicin was observed for 30 days and particle degradation was monitored by color change of the particles [22].

Camptothecin was loaded into composites of PSi and poly(l-lactide) and its controlled release behavior was studied. Three different PSi and poly(l-lactide) composite formats were prepared by grafting poly(l-lactide) from PSi films via surface-initiated ring-opening polymerization, spin coating a poly(l-lactide) solution onto oxidized PSi films and the third composite consisted of a melt-cast poly(l-lactide) monolith containing dispersed PSi microparticles. PSi grafted with thin films of poly(l-lactide) showed substantial burst release with effective for release periods of less than 24 hours. PSi films with spin coated poly(l-lactide) solution displayed slower camptothecin release for more than 1 week. Monoliths with camptothecin loaded into PSi microparticles showed slower release and can be used for drug release over time frames of more than 1 month [112].

PSi films were fabricated and surface modified by thermal hydrosilylation of 1-dodecene and undecylenic acid for loading of anti cancer drug mitoxantrone dihydrochloride. These surface chemistries had significant effect on the drug loading efficacy and the release behavior of drug molecules. The dodecyl terminated PSi exhibited sustained release over a period of a couple of days whereas native PSi showed an accelerated drug release completed within 5 hours. The undecylenic acid modified PSi in which the drug was covalently attached to the Si surface showed a continuous slower release up to 25 days with no burst effect [109].

Ocular drug delivery to the posterior segment of the eye remains a challenging task due to the diffi-

culty of crossing the blood-retinal barrier. Hydrosilylated and oxidized PSi microparticles was prepared for covalent grafting of daunorubicin for sustained ocular drug delivery system [140,141]. Daunorubicin can be used for inhibition of proliferative vitreoretinopathy formation. However, it has a short vitreous half-life in the eye and a narrow therapeutic concentration range. Hydrosilylated PSi microparticles loaded with daunorubicin shows sustained release with no ocular toxicity in a 6-month safety study in rabbit eye. However, PSi formulation was found to induce chemical degradation of the daunorubicin payload, which was attributed to the presence of residual Si-H species and elemental silicon in the particles [140]. The degradation of daunorubicin can be avoided by complete oxidation of PSi surface before drug loading. The oxidized PSi microparticles can be further modified by a silanol based linker (3-aminopropyltrimethoxysilane) to attach daunorubicin via covalent attachment. The drug release from oxidized PSi particles showed extended drug release upto 3 months with no ocular toxicity [141].

8. DRUG RELEASE KINETICS

In order to define a model which will represent a better fit for the drug delivery system, drug release data from PSi carriers can be further analyzed by different models. Higuchi and Korsmeyer-Peppas model are the most frequently used to fit a drug release profiles from PSi [112,116,122,143]. Higuchi model describes a drug release as a diffusion process based on Fick's law, square root of time release kinetics [144]. A simplified Higuchi expression based on these hypotheses can be written in the following form:

$$M_t = kt^{1/2}, \tag{4}$$

where M_t is the amount of a drug released at time t, and k is the Higuchi dissolution constant. The dissolution data from PSi loaded with poorly soluble drug itraconazole (ITZ) was fitted to Higuchi model in two-step drug release profile. This two step drug release is attributed to the faster release of drug from nearby surface of porous matrix in the first step followed by slower release of drug molecules packed deeper inside of matrix in the second step [122].

Similarly, camptothecin release profile from grafted PSi-poly(l-lactide) composites showed very good two step drug release fitting to Higuchi model. This was attributed to the diffusion controlled release in first phase followed by degradation and composite dissolution based release in the second phase. However, camptothecin release profile from spin-coated PSi composite material displayed linear fitting for full profile indicating the diffusion controlled release from these more stable composite materials [112].

Korsmeyer-Peppas model is generally applied when the drug release mechanism is not known or when there are more than one release mechanisms involved [145,146]. Korsmeyer-Peppas model is a simple, semi-empirical model, correlating exponentially the drug release to the time:

$$\frac{M_t}{M_\infty} = kt^n, \tag{5}$$

where M_t and M_∞ are the cumulative amounts of drug released at time t and infinite time, respectively; k is a constant, and n is the diffusional exponent which is indicative of the transport mechanism. The value of exponent n is determined from initial 60% of drug released. For sphere geometry, $n \leq 0.43$ indicates Fickian diffusion, $0.43 < n < 0.85$ indicate an anomalous behaviour (non-Fickian kinetics corresponding to coupled diffusion), and $n = 0.85$ indicates Case-II transport drug release [145,146].

The Korsmeyer-Peppas fitting was carried out for ibuprofen release profiles from TUD-1, SBA-15, MCM-41, and thermally carbonized PSi [116]. A very high R^2 values between 0.9924 and 0.9996 was obtained suggesting excellent fitting with Korsmeyer-Peppas model. The kinetic constant values k obtained from the Korsmeyer-Peppas model was highest for the TUD-1 material indicating fastest ibuprofen release due to its highly accessible random 3D mesopore network. The exponent n values for SBA-15 and MCM-41 were between 0.62-0.79 indicating steric hindrance caused by the long unidirectional mesopore channels for the diffusion of drug while lower n values of 0.59-0.64 were obtained for the TUD-1 material because of better accessible pore network. The n values for thermally carbonized PSi were between 0.91-1.16 suggesting deviation from purely diffusion controlled Fickian transport of drug [116].

9. CONCLUSIONS

PSi has number of unique properties applicable for drug delivery applications. PSi can be prepared by easy top-down fabrication using electrochemical etching of silicon wafers. The etching procedure allows tuning of porosity, pore size, surface area, and free volume. Pores of different sizes from micro to macropores can be easily prepared by varying cur-

rent density, electrolyte concentration, type and concentration of dopant, and crystalline orientation of Si wafer. PSi has been extensively studied for biomedical applications due to its biocompatibility, biodegradability, low toxicity, and solubility. PSi has shown good biocompatibility in biological systems without causing any undesirable side effects. PSi films can be fractured by different methods, for example, ultrasonication, ball milling, or jet milling to micro- or nanoparticles. Surface chemistry plays an important role in drug loading, drug release, and degradation of PSi matrix. The surface of freshly etched PSi can be stabilized by oxidation, hydrosilylation, and thermal carbonization for loading and release of small poorly soluble drugs, large hydrophilic drugs, anticancer drugs, or proteins. The modified surface chemistry leads to increase in dissolution of poorly soluble drugs and controlled delivery of drug molecules. The drug loading into PSi has increased the poor dissolution and poor permeation properties of various hydrophobic drugs. The optical properties of PSi have been exploited for the development of observable drug delivery system. *In vitro* and *in vivo* studies of PSi based carriers have shown excellent results for advanced drug delivery system. In future, human trials of PSi based formulations needs to be addressed using results obtained from pre clinical studies.

REFERENCES

[1] A. Uhlir // *Bell Syst. Tech. J.* **35** (1956) 333.
[2] L.T. Canham // *Appl. Phys. Lett.* **57** (1990) 1046.
[3] L.T. Canham // **7** (1995) 1033.
[4] L.T. Canham, J.P. Newey, C.L. Reeves, M.R. Houlton, A. Loni, A.J. Simons and T.I. Cox // *Adv. Mater.* **8** (1996) 847.
[5] L.T. Canham, C.L. Reeves, J.P. Newey, M.R. Houlton, T.I. Cox, J.M. Buriak and M.P. Stewart // *Adv. Mater.* **11** (1999) 1505.
[6] A. Foucaran, F. Pascal-Delannoy, A. Giani, A. Sackda, P. Combette and A. Boyer // *Thin Solid Films* **297** (1997) 317.
[7] M.J. Sailor and J.R. Link // *Chem. Commun.* (2005) 1375.
[8] S. Chan, P.M. Fauchet, Y. Li, L.J. Rothberg and B.L. Miller // *Phys. Status Solidi A* **182** (2000) 541.
[9] V.S.Y. Lin, K. Motesharei, K.S. Dancil, M.J. Sailor and M.R. Ghadiri // *Science* **278** (1997) 840.
[10] L. Gu, D.J. Hall, Z. Qin, E. Anglin, J. Joo, D.J. Mooney, S.B. Howell and M.J. Sailor // *Nat. Commun.* **4** (2013) 1.
[11] E. Tasciotti, X. Liu, R. Bhavane, K. Plant, A.D. Leonard, B.K. Price, M.M. Cheng, P. Decuzzi, J.M. Tour, F. Robertson and M. Ferrari // *Nat. Nanotechnol.* **3** (2008) 151.
[12] F. Cunin, T.A. Schmedake, J.R. Link, Y.Y. Li, J. Koh, S.N. Bhatia and M.J. Sailor // *Nat. Mater.* **1** (2002) 39.
[13] M.A. Whitehead, D. Fan, P. Mukherjee, G.R. Akkaraju, L.T. Canham and J.L. Coffer // *Tissue Eng. Part A* **14** (2008) 195.
[14] N.H. Maniya, S.R. Patel and Z.V.P. Murthy // *Superlattice. Microst.* **85** (2015) 34.
[15] N.H. Maniya, S.R. Patel and Z.V.P. Murthy // *Chem. Eng. Res. Des.* (2015), http://dx.doi.org/10.1016/j.cherd.2015.09.008.
[16] J. Salonen, L. Laitinen, A.M. Kaukonen, J. Tuura, M. Bjorkqvist, T. Heikkila, K.V. Heikkila, J. Hirvonen and V.P. Lehto // *J. Control. Release* **108** (2005) 362.
[17] J. Salonen, A.M. Kaukonen, J. Hirvonen and V.P. Lehto // *J. Pharm. Sci.* **97** (2008) 632.
[18] N.H. Maniya, S.R. Patel and Z.V.P. Murthy // *Appl. Surf. Sci.* **330** (2015) 358.
[19] X.G. Zhang // *J. Electrochem. Soc.* **151** (2004) C69.
[20] J.M. Buriak // *Chem. Rev.* **102** (2002) 1272.
[21] N.H. Maniya, S.R. Patel and Z.V.P. Murthy // *Superlattice. Microst.* **55** (2013) 144.
[22] E.C. Wu, J.S. Andrew, L. Cheng, W.R. Freeman, L. Pearson and M.J. Sailor // *Biomaterials* **32** (2011) 1957.
[23] S.C. Bayliss, L.D. Buckberry, P.J. Harris and M. Tobin // *J. Porous Mater.* **7** (2000) 191.
[24] A.B. Foraker, R.J. Walczak, M.H. Cohen, T.A. Boiarski, C.F. Grove and P.W. Swaan // *Pharm. Res.* **20** (2003) 110.
[25] L.T. Canham // *Nanotechnology* **18** (2007) 1.
[26] L. Cheng, E. Anglin, F. Cunin, D. Kim, M.J. Sailor, I. Falkenstein, A. Tammewar and W.R. Freeman // *Br. J. Ophthalmol.* **92** (2008) 705.
[27] S.P. Low, N.H. Voelcker, L.T. Canham and K.A. Williams // *Biomaterials* **30** (2009) 2873.
[28] R.J. Archer // *J. Phys. Chem. Solids* **14** (1960) 104.
[29] M.T. Kelly, J.K.M. Chun and A.B. Bocarsly // *Appl. Phys. Lett.* **64** (1994) 1693.
[30] N. Noguchi and I. Suemune // *J. Appl. Phys.* **75** (1994) 4765.
[31] O.K. Andersen, T. Frello and E. Veje // *J. Appl. Phys.* **78** (1995) 6189.

[32] S. Boughaba and K. Wang // *Thin Solid Films* **497** (2006) 83.
[33] M. Saadoun, N. Mliki, H. Kaabi, K. Daoudi, B. Bessais, H. Ezzaouia and R. Bennaceur // *Thin Solid Films* **405** (2002) 29.
[34] R.E. Hummel and C. Sung-Sik // *Appl. Phys. Lett.* **61** (1992) 1965.
[35] V. Lehmann and U. Gosele // *Appl. Phys. Lett.* **58** (1991) 856.
[36] V. Lehmann and U. Gosele // *Adv. Mater.* **4** (1992) 114.
[37] C. Levy-Clement, A. Lagoubi and M. Tomkiewicz // *J. Electrochem. Soc.* **141** (1994) 958.
[38] L. Canham, In: *EMIS Datareviews*, ed. by B.L. Weiss (Institution of Engineering and Technology, London, 1997), Vol.18, p. 1.
[39] J. Jakubowicz // *Superlattice. Microst.* **41** (2007) 205.
[40] H. Koyama, N. Shima and N. Koshida // *Phys. Rev. B* **53** (1996) R13291.
[41] M. Thonissen, M.G. Berger, R. ArensFischer, O. Gluck, M. Kruger and H. Luth // *Thin Solid Films* **276** (1996) 21.
[42] O. Bisi, S. Ossicini and L. Pavesi // *Surf. Sci. Rep.* **38** (2000) 1.
[43] G. Vincent // *Appl. Phys. Lett.* **64** (1994) 2367.
[44] C. Mazzoleni and L. Pavesi // *Appl. Phys. Lett.* **67** (1995) 2983.
[45] M.G. Berger, R. Arens-Fischer, M. Thoenissen, M. Kruger, S. Billat, H. Luth, S. Hilbrich, W. Theiß and P. Grosse // *Thin Solid Films* **297** (1997) 237.
[46] N.H. Maniya, S.R. Patel and Z.V.P. Murthy // *Optik* **125** (2014) 828.
[47] S.H.C. Anderson, H. Elliott, D.J. Wallis, L.T. Canham and J.J. Powell // *Phys. Status Solidi A* **197** (2003) 331.
[48] M.J. Sailor, *Porous Silicon in Practice, first edition* (Wiley-VCH, Weinheim, 2011).
[49] E. Segal, L.A. Perelman, F. Cunin, F.D. Renzo, J.M. Devoisselle, Y.Y. Li and M.J. Sailor // *Adv. Funct. Mater.* **17** (2007) 1153.
[50] R. Herino, G. Bomchil, K. Barla, C. Bertrand and J.L. Ginoux // *J. Electrochem. Soc.* **134** (1987) 1994.
[51] J.L. Heinrich, C.L. Curtis, G.M. Credo, K.L. Kavanagh and M.J. Sailor // *Science* **255** (1992) 66.
[52] L.M. Bimbo, M. Sarparanta, H.A. Santos, A.J. Airaksinen, E. Makila, T. Laaksonen, L. Peltonen, V.P. Lehto, J. Hirvonen and J. Salonen // *ACS Nano* **4** (2010) 3023.
[53] Z. Qin, J. Joo, L. Gu and M.J. Sailor // *Part. Part. Syst. Charact.* **31** (2014) 252.
[54] S.O. Meade, M.S. Yoon, K.H. Ahn and M.J. Sailor // *Adv. Mater.* **16** (2004) 1811.
[55] Y.Y. Li, V.S. Kollengode and M.J. Sailor // *Adv. Mater.* **17** (2005) 1249.
[56] J. Salonen, V.P. Lehto and E. Laine // *Appl. Surf. Sci.* **120** (1997) 191.
[57] E.C. Wu, J.S. Andrew, A. Buyanin, J.M. Kinsella and M.J. Sailor // *Chem. Commun.* **47** (2011) 5699.
[58] K.L. Jarvis, T.J. Barnes and C.A. Prestidge // *Langmuir* **26** (2010) 14316.
[59] K.P.S. Dancil, D.P. Greiner and M.J. Sailor // *J. Am. Chem. Soc.* **121** (1999) 7925.
[60] J.H. Song and M.J. Sailor // *Inorg. Chem.* **37** (1998) 3355.
[61] G. Mattei, E.V. Alieva, J.E. Petrov and V.A. Yakovlev // *Phys. Status Solidi A* **182** (2000) 139.
[62] N.H. Maniya, S.R. Patel and Z.V.P. Murthy // *Mater. Res. Bull.* **57** (2014) 6.
[63] K.L. Jarvis, T.J. Barnes and C.A. Prestidge // *Adv. Colloid Interface Sci.* **175** (2012) 25.
[64] R. Boukherroub, S. Morin, D.D.M. Wayner and D.J. Lockwood // *Phys. Status Solidi A* **182** (2000) 117.
[65] R. Boukherroub, A. Petit, A. Loupy, J.N. Chazalviel and F. Ozanam // *J. Phys. Chem. B* **107** (2003) 13459.
[66] R. Boukherroub, J.T.C. Wojtyk, D.D.M. Wayner and D.J. Lockwood // *J. Electrochem. Soc.* **149** (2002) 59.
[67] M.P. Stewart and J.M. Buriak // *Angew. Chem. Int. Ed. Engl.* **37** (1998) 3257.
[68] M.P. Stewart and J.M. Buriak // *J. Am. Chem. Soc.* **123** (2001) 7821.
[69] J.M. Buriak and M.J. Allen // *J. Am. Chem. Soc.* **120** (1998) 1339.
[70] J. Chapron, S.A. Alekseev, V. Lysenko, V.N. Zaitsev and D. Barbier // *Sensor. Actuat. B: Chem* **120** (2007) 706.
[71] K.A. Kilian, T. Boecking and J.J. Gooding // *Chem. Commun.* **6** (2009) 630.
[72] M. Warntjes, C. Vieillard, F. Ozanam and J.N. Chazalviel // *J. Electrochem. Soc.* **142** (1995) 4138.
[73] V.M. Dubin, C. Vieillard, F. Ozanam and J.N. Chazalviel // *Phys. Status Solidi A* **190** (1995) 47.
[74] F. Erogbogbo, K.T. Yong, I. Roy, G.X. Xu, P.N. Prasad and M.T. Swihart // *ACS Nano* **2** (2008) 873.

[75] N.Y. Kim and P.E. Laibinis // *J. Am. Chem. Soc.* **120** (1998) 4516.
[76] M.R. Linford, P. Fenter, P.M. Eisenberger and C.E.D. Chidsey // *J. Am. Chem. Soc.* **117** (1995) 3145.
[77] J. Terry, M.R. Linford, C. Wigren, R. Cao, P. Pianetta and C.E.D. Chidsey // *Appl. Phys. Lett.* **71** (1997) 1056.
[78] J.H. Song and M.J. Sailor // *J. Am. Chem. Soc.* **120** (1998) 2376.
[79] T. Dubois, F. Ozanam and J.N. Chazalviel, In: *Proceedings of Electrochemical Society* (Canada, Montreal, Quebec, 1997), PAGE????.
[80] C.H. deVilleneuve, J. Pinson, M.C. Bernard and P. Allongue // *J. Phys. Chem. B* **101** (1997) 2415.
[81] C. Gurtner, A.W. Wun and M.J. Sailor // *Angew. Chem. Int. Ed.* **38** (1999) 1966.
[82] I.N. Lees, H. Lin, C.A. Canaria, C. Gurtner, M.J. Sailor and G.M. Miskelly // *Langmuir* **19** (2003) 9812.
[83] J. Salonen, V.P. Lehto, M. Bjorkqvist, E. Laine and L. Niinisto // *Phys. Status Solidi A* **182** (2000) 123.
[84] J. Salonen, E. Laine and L. Niinisto // *J. Appl. Phys.* **91** (2002) 456.
[85] M. Bjorkqvist, J. Salonen, E. Laine and L. Niinisto // *Phys. Status Solidi A* **197** (2003) 374.
[86] M. Bjorkqvist, J. Salonen, J. Paski and E. Laine // *Sensor. Actuat. A: Phys* **112** (2004) 244.
[87] J. Salonen, M. Bjorkqvist, E. Laine and L. Niinisto // *Appl. Surf. Sci.* **225** (2004) 289.
[88] K.A. Kilian, T. Bocking, K. Gaus, M. Gal and J.J. Gooding // *Biomaterials* **28** (2007) 3055.
[89] M.P. Schwartz, F. Cunin, R.W. Cheung and M.J. Sailor // *Phys. Status Solidi A* **202** (2005) 1380.
[90] A.S. Anderson, A.M. Dattelbaum, G.A. Montano, D.N. Price, J.G. Schmidt, J.S. Martinez, W.K. Grace, K.M. Grace and B.I. Swanson // *Langmuir* **24** (2008) 2240.
[91] A.J. Nijdam, M.M.C. Cheng, D.H. Geho, R. Fedele, P. Herrmann, K. Killian, V. Espina, E.F. Petricoin, L.A. Liotta and M. Ferrari // *Biomaterials* **28** (2007) 550.
[92] A. Janshoff, K.P.S. Dancil, C. Steinem, D.P. Greiner, V.S.Y. Lin, C. Gurtner, K. Motesharei, M.J. Sailor and M.R. Ghadiri // *J. Am. Chem. Soc.* **120** (1998) 12108.
[93] S.C. Bayliss, R. Heald, D.I. Fletcher and L.D. Buckberry // *Adv. Mater.* **11** (1999) 318.
[94] L.M. Karlsson, M. Schubert, N. Ashkenov and H. Arwin // *Thin Solid Films* **455-456** (2004) 726.
[95] T. Jay, L.T. Canham, K. Heald, C.L. Reeves and R. Downing // *Phys. Status Solidi A* **182** (2000) 555.
[96] F. Johansson, M. Kanje, C.E. Linsmeier and L. Wallman // *IEEE Trans. Biomed. Eng.* **55** (2008) 1447.
[97] S.D. Alvarez, A.M. Derfus, M.P. Schwartz, S.N. Bhatia and M.J. Sailor // *Biomaterials* **30** (2009) 26.
[98] J.H. Park, L. Gu, G. von Maltzahn, E. Ruoslahti, S.N. Bhatia and M.J. Sailor // *Nat. Mater.* **8** (2009) 331.
[99] M.A. Tolli, M.P.A. Ferreira, S.M. Kinnunen, J. Rysa, E.M. Makila, Z. Szabo, R.E. Serpi, P.J. Ohukainen, M.J. Valimaki, A.M.R. Correia, J.J. Salonen, J.T. Hirvonen, H.J. Ruskoaho and H.A. Santos // *Biomaterials* **35** (2014) 8394.
[100] H.A. Santos, J. Riikonen, J. Salonen, E. Makila, T. Heikkila, T. Laaksonen, L. Peltonen, V.P. Lehto and J. Hirvonen // *Acta Biomater.* **6** (2010) 2721.
[101] M. Steinert, J. Acker, A. Henssge and K. Wetzig // *J. Electrochem. Soc.* **152** (2005) C843.
[102] C.A. Caras, J.M. Reynard and F.V. Bright // *Appl. Spectrosc.* **67** (2013) 570.
[103] S.M. Haidary, E.P. Corcoles and N.K. Ali // *J. Nanomater.* **2012** (2012) 1.
[104] J.R. Dorvee, A.M. Derfus, S.N. Bhatia and M.J. Sailor // *Nat. Matter.* **3** (2004) 896.
[105] G. Mattei, V. Valentini and V.A. Yakovlev // *Surf. Sci.* **502** (2002) 58.
[106] N.L. Fry, G.R. Boss and M.J. Sailor // *Chem. Mater.* **26** (2014) 2758.
[107] J.S. Andrew, E.J. Anglin, E.C. Wu, M.Y. Chen, L. Cheng, W.R. Freeman and M.J. Sailor // *Adv. Funct. Mater.* **20** (2010) 4168.
[108] E.J. Anglin, M.P. Schwartz, V.P. Ng, L.A. Perelman and M.J. Sailor // *Langmuir* **20** (2004) 11264.
[109] A. Tzur-Balter, A. Gilert, N. Massad-Ivanir and E. Segal // *Acta Biomater.* **9** (2013) 6208.
[110] S. Kashanian, F. Harding, Y. Irani, S. Klebe, K. Marshall, A. Loni, L. Canham, D. Fan, K.A. Williams, N.H. Voelcker and J.L. Coffer // *Acta Biomater.* **6** (2010) 3566.
[111] K. Nan, F. Ma, H. Hou, W.R. Freeman, M.J. Sailor and L. Cheng // *Acta Biomater.* **10** (2014) 3505.

[112] S.J. McInnes, Y. Irani, K.A. Williams and N.H. Voelcker // *Nanomedicine* **7** (2012) 995.
[113] J. Hernandez-Montelongoa, N. Naveasa, S. Degoutinb, N. Tabary, F. Chai, V. Spampinato, G. Ceccone, F. Rossi, V. Torres-Costa, M. Manso-Silvana and B. Martel // *Carbohydr. Polym.* **110** (2014) 238.
[114] J. Ji, F.E.H. Tay, J. Miao and C. Iliescu // *J. Micromech. Microeng.* **16** (2006) 958.
[115] J. Ji, F.E.H. Tay, J. Miao and C. Iliescu // *J. Phys. Conf. Ser.* **34** (2006) 1127.
[116] T. Heikkila, J. Salonen, J. Tuura, N. Kumar, T. Salmi, D.Y. Murzin, M.S. Hamdy, G. Mul, L. Laitinen, A.M. Kaukonen, J. Hirvonen and V.P. Lehto // *Drug Deliv.* **14** (2007) 337.
[117] A.M. Kaukonen, L. Laitinen, J. Salonen, J. Tuura, T. Heikkila, T. Limnell, J. Hirvonen and V.P. Lehto // *Eur. J. Pharm. Biopharm.* **66** (2007) 348.
[118] L.M. Bimbo, E. Makila, T. Laaksonen, V.P. Lehto, J. Salonen, J. Hirvonen and H.A. Santos // *Biomaterials* **32** (2011) 2625.
[119] T. Limnell, J. Riikonen, J. Salonen, A. Kaukonen, L. Laitinen, J. Hirvonen and V.P. Lehto // *Int. J. Pharm.* **343** (2007) 141.
[120] F. Wang, H. Hui, T.J. Barnes, C. Barnett and C.A. Prestidge // *Mol. Pharm.* **7** (2010) 227.
[121] M. Tahvanainen, T. Rotko, E. Makila, H.A. Santos, D. Neves, D.T. Laaksonen, A. Kallonen, K. Hamalainen, M. Peura, R. Serimaa, J. Salonen, J. Hirvonen and L. Peltonen // *Int. J. Pharm.* **422** (2012) 125.
[122] P. Kinnari, E. Makila, T. Heikkila, J. Salonen, J. Hirvonen and H.A. Santos // *Int. J. Pharm.* **414** (2011) 148.
[123] N. Vale, E. Makila, J. Salonen, P. Gomes, J. Hirvonen and H.A. Santos // *Eur. J. Pharm. Biopharm.* **81** (2012) 314.
[124] T. Tanaka, L.S. Mangala, P.E. Vivas-Mejia, R. Nieves-Alicea, A.P. Mann, E. Mora, H.D. Han, M.K. Mian Shahzad, X. Liu, R. Bhavane, J. Gu, J.R. Fakhoury, C. Chiappini, C. Lu, K. Matsuo, B. Godin, R.L. Stone, A.M. Nick, G. Lopez-Berestein, A.K. Sood and M. Ferrari // *Cancer Res.* **70** (2010) 3687.
[125] L.M. Bimbo, O.V. Denisova, E. Makila, M. Kaasalainen, J.K. De Brabander, J. Hirvonen, J. Salonen, L. Kakkola, D. Kainov and H.A. Santos // *ACS Nano* **7** (2013) 6884.
[126] M. Wang, J.L. Coffer, K. Dorraj, P.S. Hartman, A. Loni and L.T. Canham // *Mol. Pharm.* **7** (2010) 2232.
[127] L. Tang, A. Saharay, W. Fleischer, P.S. Hartman, A. Loni, L.T. Canham and J.L. Coffer // *Silicon* **5** (2013) 213.
[128] L.M. Karlsson, P. Tengvall, I. Lundström and H. Arwin // *J. Colloid Interface Sci.* **266** (2003) 40.
[129] C.A. Prestidge, T.J. Barnes, A. Mierczynska-Vasilev, W. Skinner, F. Peddie and C. Barnett // *Phys. Status Solidi A* **204** (2007) 3361.
[130] M. Kilpelainen, J. Monkare, M.A. Vlasova, J. Riikonen, V.P. Lehto, J. Salonen, K. Jarvinen and K.H. Herzig // *Eur. J. Pharm. Biopharm.* **77** (2011) 20.
[131] M. Kovalainen, J. Monkare, M. Kaasalainen, J. Riikonen, V.P. Lehto, J. Salonen, K.H. Herzig and K. Jarvinen // *Mol. Pharm.* **10** (2013) 353.
[132] D. Liu, L.M. Bimbo, E. Makila, F. Villanova, M. Kaasalainen, B. Herranz-Blanco, C.M. Caramella, V.P. Lehto, J. Salonen, K.H. Herzig, J. Hirvonen and H.A. Santos // *J. Control. Release* **170** (2013) 268.
[133] M. Kilpelainen, J. Riikonen, M.A. Vlasova, A. Huotari, V.P. Lehto, J. Salonen, K.H. Herzig and K. Jarvinen // *J. Control. Release* **137** (2009) 166.
[134] A. Huotari, W. Xu, J. Monkare, M. Kovalainen, K.H. Herzig, V.P. Lehto and K. Jarvinen // *Int. J. Pharm.* **454** (2013) 67.
[135] F. Araujo, N. Shrestha, M.A. Shahbazi, P. Fonte, E.M. Makila, J.J. Salonen, J.T. Hirvonen, P.L. Granja, H.A. Santos and B. Sarmento // *Biomaterials* **35** (2014) 9199.
[136] X. Li, J.S. John, J.L. Coffer, Y. Chen, R.F. Pinizzotto, J. Newey, C. Reeves and L.T. Canham // *Biomed. Microdevices* **2** (2000) 265.
[137] J.S. Park, J.M. Kinsella, D.D. Jandial, S.B. Howell and M.J. Sailor // *Small* **7** (2011) 2061.
[138] L. Vaccari, D. Canton, N. Zaffaroni, R. Villa, M. Tormen and E. di Fabrizio // *Microelectron. Eng.* **83** (2006) 1598.
[139] E.C. Wu, J.H. Park, J. Park, E. Segal, F. Cunin and M.J. Sailor // *ACS Nano* ***2*** (2008) 2401.

[140] K.I. Hartmann, A. Nieto, E.C. Wu, W.R. Freeman, J.S. Kim, J. Chhablani, M.J. Sailor and L. Cheng // *J. Ocul. Pharmacol. Ther.* **29** (2013) 493.
[141] J. Chhablani, A. Nieto, H.Y. Hou, E.C. Wu, W.R. Freeman, M.J. Sailor and L. Cheng // *Invest. Ophthalmol. Vis. Sci.* **54** (2013) 1268.
[142] H. Hou, A. Nieto, F. Ma, W.R. Freeman, M.J. Sailor and L. Cheng // *J. Control. Release* **178** (2014) 46.
[143] J. Andersson, J. Rosenholm, S. Areva and M. Linden // *Chem. Mater.* **16** (2004) 4160.
[144] T. Higuchi // *J. Pharm. Sci.* **50** (1961) 874.
[145] R.W. Korsmeyer, R. Gurny, E.M. Doelker, P. Buri and N.A. Peppas // *Int. J. Pharm.* **15** (1983) 25.
[146] P. Costa and J.M. Sousa Lobo // *Eur. J. Pharm. Sci.* **13** (2001) 123.